International Journal of Technology (2016) 8: 1291-1300
ISSN 2086-9614

A STUDY OF THE STRUCTURAL AND ELECTROCHEMICAL PROPERTIES OF Li_3PO_4-MMT-PVDF COMPOSITES FOR SOLID ELECTROLYTES

H. Jodi[1,2*], Anne Zulfia[2], Deswita[1], E. Kartini[1]

[1]*Center for Science and Technology of Advanced Materials, BATAN, Kawasan Puspiptek, Serpong, Tangerang, Banten 15314, Indonesia*
[2]*Department of Metallurgy and Materials Engineering, Faculty of Engineering, Universitas Indonesia, Kampus UI Depok, Depok 16424, Indonesia*

(Received: November 2016 / Revised: December 2016 / Accepted: December 2016)

ABSTRACT

Batteries on the market today still use liquid-type electrolytes, which can result in safety issues caused by electrolyte leakage. Therefore, studies that search for solid-state electrolytes are important for resolving these issues. In this research, a composite of lithium phosphate-montmorillonite-polyvinylidene fluoride (Li_3PO_4-MMT-PVDF) has been characterized with the aim of detecting the electrochemical performance of Li_3PO_4 with the addition of MMT. Li_3PO_4 samples were prepared through a solid-state reaction, which was then mixed with MMT, which had a composition ranging from 5 wt% to 20 wt%, and 1 wt% PVDF as a binder. This characterization was conducted with structural, morphological, and electrochemical aspects. The structural test showed that the X-ray diffraction (XRD) pattern was dominated by Li_3PO_4 peaks and MMT aluminosilicates. The electrochemical characterization indicated that the conductivity value of the composites was greater than that of Li_3PO_4. The highest conductivity was achieved with a 15 wt% MMT addition, with a dielectric-constant value of 74.9 at a frequency of 10 kHz.

Keywords: Composites; Electrochemical Impedance Spectroscopy; Lithium Phosphate; Montmorillonite; Solid Electrolyte

1. INTRODUCTION

Increased use of electronic devices necessitates further research and the discovery of new batteries. One of the main components in a battery is the electrolyte, which is a medium for delivering ions in between electrodes. Usually, the electrolytes of a battery consist of dissolved lithium salt in an organic solvent. Liquid electrolytes cause an irreversible loss of battery capacity that cannot be regained; they also prevent any increase in the battery lifecycle, restrict the temperature range for battery usage, and induce leakage and security issues (Kotobuki, 2012). Because of these problems, the substitution of liquid electrolytes with a solid form is an interesting and important issue.

The solid-type electrolytes hold the potential to be applied in a wide variety of electrochemical devices, such as the solid-state battery, sensors, and capacitors, and such devices are expected to unravel the problems associated with loss of capacity, duration of lifespan, security, and temperature ranges, as described above (Sahu et al., 2014). Solid electrolytes do not cause leakage or pollution, and they have better resistance to shock and vibration compared to liquid

*Corresponding author's email: herieldi@batan.go.id, herieldi@gmail.com, Tel. +62-21-7562860, Fax. +62-21-7560926
Permalink/DOI: https://doi.org/10.14716/ijtech.v7i8.6894

electrolytes (Fergus, 2010). The solid electrolyte is also a single-ion conductor, which means only one species of carrier can be transmitted. Therefore, during its employment, there is almost no concentration gradient in the cell, and the solid electrolyte is useful for reducing the potency of cell overpotential (Quartarone & Mustarelli, 2011).

Lithium phosphate (Li_3PO_4) is a polymorph of Li_2O-P_2O_5 systems, and it is one of the best, most stable solid electrolytes ever made. This material has a sufficiently low conductivity to be applied to a battery, caused by high bulk resistance, so Li_3PO_4 solid-electrolyte materials are widely used in the form of a thin layer to reduce the resistance value (Ribeiro et al., 2012; Senevirathne et al., 2013). Not only are solid-electrolyte-based phosphate oxide materials easy to prepare, but they also have a strong glass-forming character, low melting point, and simple composition. Previous research has proposed phosphate-oxide-based material as a solid-state electrolyte (Jodi et al., 2016; Kartini et al., 2014; Nur et al., 2016). Investigations of the structures and Li^+ ion diffusion mechanisms in idealized Li_3PO_4 crystals have previously been reported in works involving first-principles modeling techniques (Lepley & Holzwarth, 2012).

Many studies have aimed to increase the conductivity of phosphate-oxide-based conductors. Some of these approaches include mixing two or more different kinds of anion to form a mixed-anion effect (Raguenet et al., 2012). Modifications that added Al_2O_3 and TiO_2 to the Li_2O-P_2O_5 system produced a new Li_2O-Al_2O_3-Ti_2O-P_2O_5 (LATP) system, which is currently the most investigated. The highest conductivity achieved by this system reportedly reached a value of 1.3×10^{-3} S/cm (He et al., 2014). A further modification to the LATP system that added SiO_2 provided a conductivity value of $2\sim3\times10^{-3}$ S/cm (Yi et al., 2014). SiO_2 independently added to the Li_2O-P_2O_5 system generated a new system of $50Li_4SiO_4$-$50Li_3PO_4$, which provided the conductivity of 1.6×10^{-6} S/cm at room temperature in the form of a film; this conductivity is higher than those of Li_3PO_4 and Li_4SiO_4 films. The coating of this film on the electrode was effective in lowering electrode–electrolyte interfacial resistance and expanding the power density of the all-solid-state cells (Sakurai et al., 2011). Although modifications of the Li_2O-P_2O_5 system that add either alumina or silica have often been reported, no modifications have been conducted that add material containing alumina and silica simultaneously. In this work, montmorillonite (MMT) has been used as the material containing alumina and silica to modify the Li_2O-P_2O_5 system due to its low cost, non-toxicity, and natural abundance. Polyvinylidene fluoride solutions have been used as a binder so the new blended material can be easily molded into pellets.

MMT is a soft phyllosilicate mineral that typically forms as microcrystal clay. MMT has a sandwich structure, where a layer of octahedral alumina is sandwiched between two tetrahedral silica layers. Between these layers, there is space that can be occupied by cations that can be exchanged. MMT has a high cation-exchange capacity, so the space between the layers of MMT is able to accommodate a large number of cations. In application, MMT was reported to have been prepared as a composite-polymer electrolyte for a Li-ion battery (Deka & Kumar, 2011). The ionic liquid could be intercalated into MMT layers, which influenced the swelling effect of MMT and increased the thermal stability of the ionic liquid (Takahashi et al., 2013).

This study focuses on electrochemical characterization to determine the effect of MMT additions on the electrochemical properties of Li_3PO_4, in the form of a Li_3PO_4-MMT composite with a PVDF polymer as a binder. Synthesized samples were characterized using X-ray diffraction (XRD) and scanning electron microscopy (SEM), with energy dispersive X-ray spectroscopy (EDS) as well as electrical properties that used electrochemical impedance spectrometry (EIS). The XRD pattern confirmed a new diffraction peak for the aluminosilicate phase in the samples with an MMT addition. The morphological images showed that MMT particles filled the spaces between particles of Li_3PO_4. The highest conductivity of lithium

phosphate-montmorillonite-polyvinylidene fluoride (Li_3PO_4-MMT-PVDF) composites was attained by the sample of a 15 wt% addition of MMT.

2. EXPERIMENTAL SETUP

The materials used for this work were lithium carbonate (Li_2CO_3, Alfa Caesar, 99%), ammonium dihydrogen phosphate ($NH_4H_2PO_4$, Merck, 98%), montmorillonite (MMT K10, Sigma-Aldrich), polyvinylidene fluoride (PVDF, Sigma-Aldrich), and N-Methyl-2-pyrrolidinone (NMP, Sigma-Aldrich, 99%). Ceramic crucibles, a digital scale, a milling machine, and a heating furnace were used for preparing samples.

Li_3PO_4 was prepared using the conventional melt-quenching method. Li_2CO_3 and $NH_4H_2PO_4$ were mixed at a molar ratio of 3:2 and ground together in an agate mortar for an hour. The batches were initially kept at a temperature of up to 675°C for an hour each in order to release volatile products. Then, the batches were heated up to 775°C to form Li_3PO_4 crystals, and they were melted at that temperature for an hour. The molten mixture was quenched in liquid nitrogen and smoothed in an agate mortar.

Commercially available MMT was then mixed into the prepared Li_3PO_4 at MMT compositions of 0, 5, 10, 15, and 20 wt%. The mechanical milling treatment was carried out for each batch using a planetary ball mill at 1000 rpm for 2 hours at room temperature. PVDF powder was dissolved in the NMP solvent to form a 1%-PVDF solution, which was added to each batch at a composition of 1 wt%. The mixture was then stirred and heated in order to evaporate the solvent. Each mixture was pressed into a pellet 15 mm in diameter with a pressure of 12000 psi in an axial hole of Stainless steel dies. Samples were coded as LMP xx, where LMP stand for Lithium phosphate Montmorillonite Polyvinylidene fluoride and xx indicates the percentage of MMT added.

Crystalline phases of the samples were identified by XRD at room temperature. Shimadzu XD-610 equipped with a Cu $K_{\alpha 1}$ source target was utilized to record the XRD pattern of the samples. Diffraction patterns were logged with a goniometer (2θ) from 10° to 90°.

The morphology of the samples was observed by means of SEM on the surface of the samples. JEOL JSM-6510LA equipped with EDS was employed to observe the morphology and elemental analysis of the samples.

Electrochemical characterization was carried out for the samples using a HIOKI LCR HiTESTER 3532-50 for EIS. Silver paste, which serves as an ion-blocking electrode and current collector, was applied on both sides of the samples. Impedance spectra were collected in an ambient atmosphere and temperature at an applied voltage of 1 V over a frequency range of 42 Hz – 1 MHz.

3. RESULTS AND DISCUSSION

XRD spectra for the Li_3PO_4-MMT-PVDF composite samples are shown in Figure 1. The results show that the spectra were composed mainly of Li_3PO_4 crystals. Search and match analysis identified that the composition of Li_3PO_4 phases in all spectra was in the range of 93–100%.

The XRD pattern for the sample with no MMT additions (LMP 00) is displayed in Figure 1. The spectra were matched with the standard Li_3PO_4, which has an orthorhombic structure. According to previous research, this Li_3PO_4 pattern belongs to the γ-Li_3PO_4 phase (Jodi et al., 2016; Nur et al., 2016). The highest peak was at $2\theta = 21.9°$, with a Full width at half maximum (FWHM) value of 0.126 and a crystallite size of 554.8 Å.

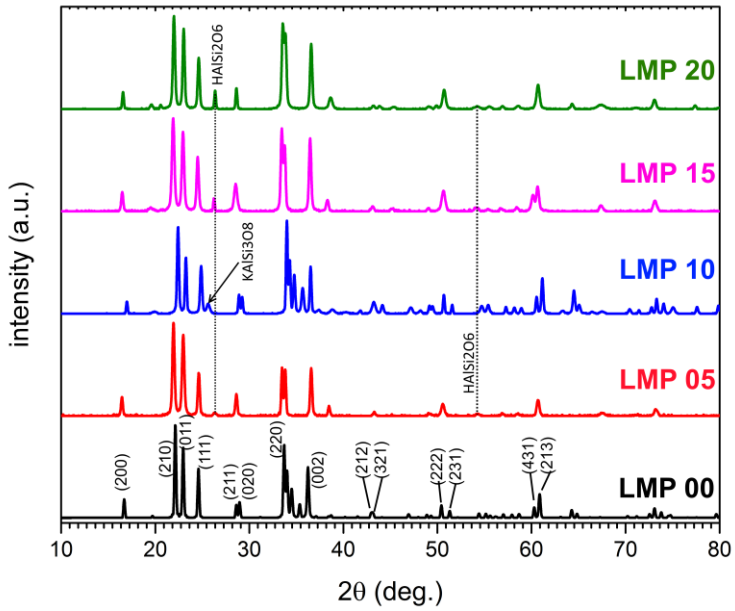

Figure 1 X-ray diffraction (XRD) pattern of Li_3PO_4-MMT-PVDF composite samples with 0, 5, 10, 15, and 20 wt% for the montmorillonite (MMT) addition

The XRD spectra from the blends of LMP 05, LMP 10, LMP 15, and LMP 20 (samples with an MMT addition) reveal a new peak at 2θ = 26.2° that was identified as a peak of $H_1Al_1Si_2O_6$ (#98-006-9215). The peak's relative intensity levels were increasing along with the incremental addition of MMT. This peak had a crystallite size that was increasing along with the MMT addition, but it reached its highest value at a 15 wt% addition, subsequently decreasing at further additions. Other peaks in this phase were detected at 2θ = 38.6°, 49.1°, 49.8°, 54.2°, 55.4°, 58.5°, 73.1°, 77.3°, and 80.5°, but these peaks were the concurrent reflection of both Li_3PO_4 and $H_1Al_1Si_2O_6$ phases. One peak indicated as an impurity was detected in the spectral data of LMP 10 at 2θ = 25.4°, and it was identified as belonging to the $K_1Al_1Si_3O_8$ phase (#98-018-4499). This impurity may come from the nature of MMT clay.

SEM micrographs of Li_3PO_4-MMT-PVDF composites with a different weight percentage of MMT are shown in Figure 2. It is clearly shown that the surface of the samples is covered by a PVDF polymer solution, which is forced to the surface by the pressure of the pelleting process (see Figure 2a).

Figure 2b clearly shows how the morphology of composites with no MMT additions provides a rough surface consisting of Li_3PO_4 particles (about 2.2–10 μm) with some porous openings. Agglomeration was observed, which may have occurred as a result of the gradually heated synthesis and the use of a liquid PVDF solution. With the addition of MMT, a decrease in surface roughness was observed with an increase of MMT up to 15 wt%, which resulted in the appearance of a smooth surface texture. These changes may be attributed to the filling of spaces at the surface level by smaller MMT particles. Upon a further addition of 20 wt% MMT, the morphology again showed a rough surface (see Figure 2f).

Quantitative analysis using EDS gave the elemental composition of the samples, which are dominated by the elements of C, O, P, and Au. The elements of C and Au originate from the PVDF solution and from the sputtered thin layer on the surface, respectively. For the blend with no MMT additions, the ratio of the atomic composition from O to P is 57.82 to 13.30, which means that, on average, the sample is dominated by Li_3PO_4. Small amounts of Si and Al were

recorded in the spot-area observation of Li_3PO_4-MMT-PVDF samples with MMT additions of 5–20 wt%.

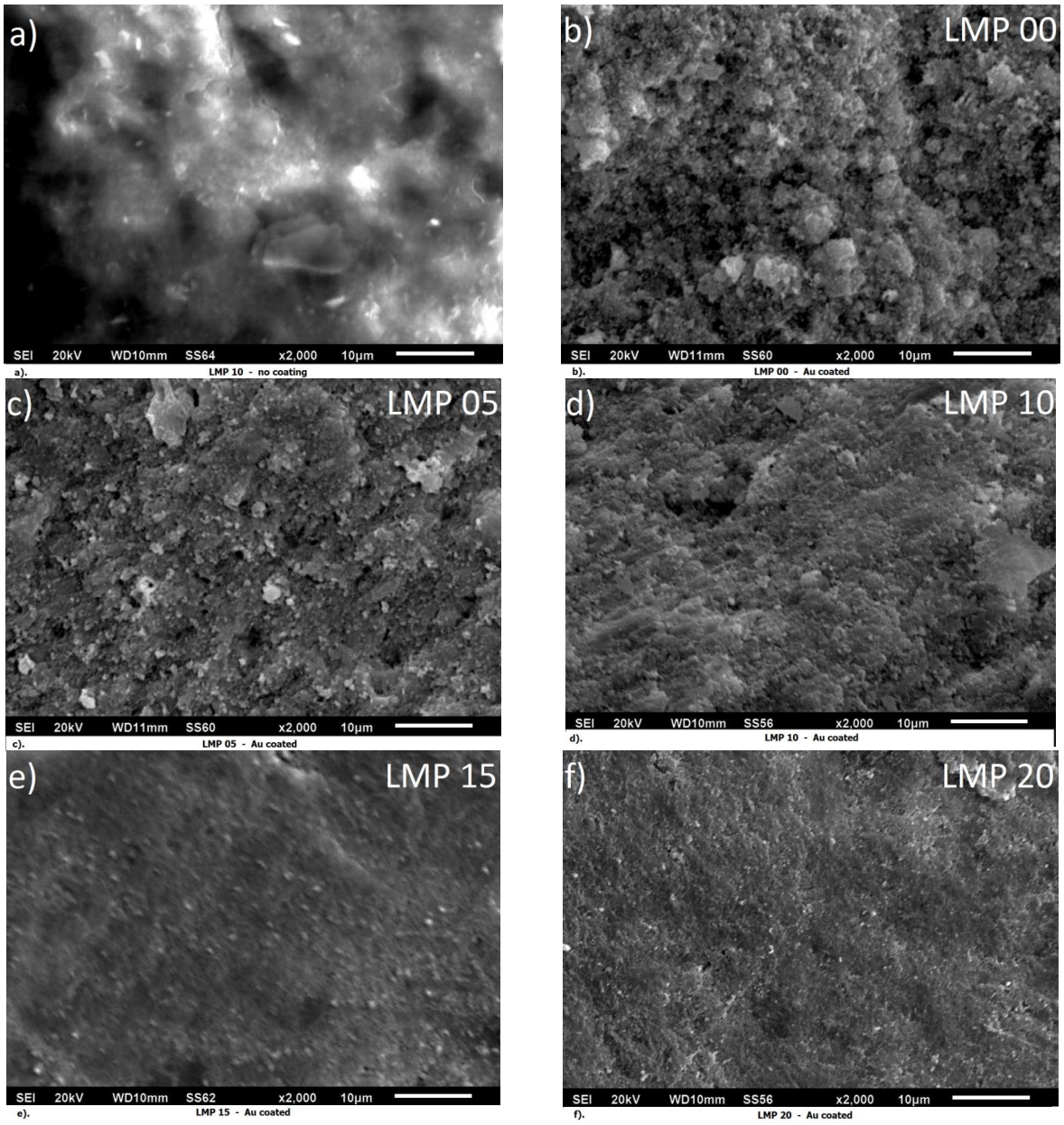

Figure 2 Scanning electron microscopy (SEM) micrographs of Li_3PO_4-MMT-PVDF composites with different wt% of montmorillonite (MMT)

The impedance plots for Li_3PO_4-MMT-PVDF composites at room temperature are presented in Figure 3. The impedance plot for the system with no MMT additions (LMP 00) consists of a small portion of a depressed semicircle, while the plots show a semicircular arc for the system with MMT additions. In addition, the impedance plot for LMP 15 shows a spike in the lower-frequency region. The high-frequency semicircular arc is attributed to the bulk properties of the electrolytes, and it can be represented as an electrical circuit consisting of a resistor (due to mobile ions) and a capacitor (due to immobile anions) in a parallel connection. The low-frequency spike is attributed to double layer capacitance due to space charge polarization at the electrode–electrolyte interface. The bulk resistance R_b of the electrolytes was obtained by the interception of an extrapolated semicircle with a real axis or with a low-frequency spike

(Chilaka & Ghosh, 2014). The value of Rb is observed to decrease by increasing the MMT addition up to 15 wt%; then, this value increases with a 20 wt% addition, as represented in Table 1.

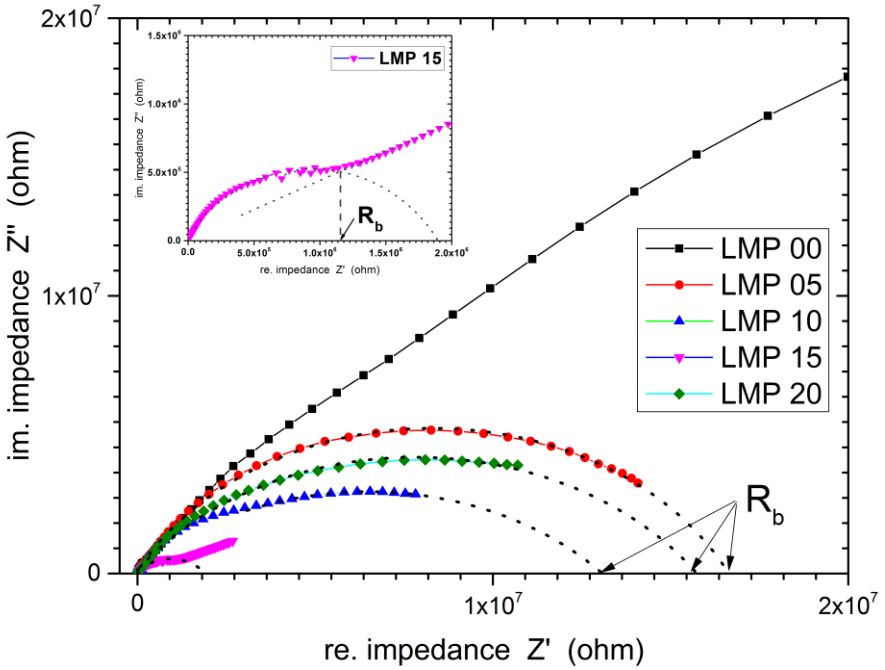

Figure 3 Room temperature complex-impedance plots (Cole-Cole Plots) for Li_3PO_4-MMT-PVDF composites with 0, 5, 10, 15, and 20 wt% of montmorillonite (MMT) additions. The inserted graph shows how to find the bulk resistance value for the system with a 15 wt% MMT addition

The conductivity of the electrolytes was calculated from the measured impedance value and dimension of the electrolytes as thickness and surface area. The complex conductivity follows Jonscher's power law and is varied with angular frequency (Jonscher, 1977):

$$\sigma(\omega)_{ac} = \sigma_{dc} + A\omega^{n}, \quad (1)$$

where σ_{dc}, A, and n are the DC conductivity, the AC conductivity parameter, and the power law exponent, respectively. The variation of complex conductivity as a function of frequency for Li_3PO_4-MMT-PVDF composites, as shown in Figure 4. It is evident that the complex conductivity is increasing with the addition of MMT up to 15 wt%, and it is decreasing with a 20 wt% MMT addition.

The conductivity plots were fitted to Jonscher's law equation using a non-linear least squares fitting procedure to extract the conductivity parameters. Fitted values are presented in Table 1. With the addition of MMT from 0 to 15 wt%, the DC conductivity of the blends is clearly observed to increase up to two orders of magnitude. The incremental increase in conductivity may be ascribed either to the increase in mobile ion concentration or to the increase of free space allowing the ions to move due to the addition of MMT. However, DC conductivity is observed to decrease at the MMT concentration of 20 wt%. This decrease may be attributed to the dominating role of ion association over free ion formation, which reduces the number of ions for conduction (Pradhan et al., 2008). The values evaluated for power law exponent n are in the range of 0.62–0.85 for all compositions of MMT, indicating that backward hopping is slower than the site relaxation time for all compositions. Consequently, the long-range drift of

ions may be one of the sources of ion conduction in the system's Li_3PO_4-MMT-PVDF composites.

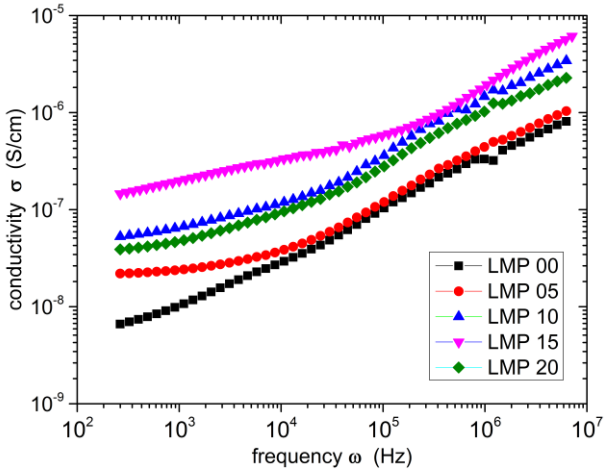

Figure 4 The room-temperature frequency-dependent plots of conductivity for Li_3PO_4-MMT-PVDF composites with montmorillonite (MMT) additions of 0, 5, 10, 15, and 20 wt%

Table 1 The bulk resistance and fitted conductivity parameters for the Li_3PO_4-MMT-PVDF composites calculated from experimental impedance and conductivity values

Frequency	Bulk resistance R_b (ohm)	DC conductivity σ_{dc} (S/cm)	AC conductivity parameter A	Power law exponent n
LMP 00	$1.06\times10^{+8}$	4.92×10^{-9}	7.45×10^{-11}	0.62
LMP 05	$1.66\times10^{+7}$	2.10×10^{-8}	1.58×10^{-11}	0.76
LMP 10	$1.31\times10^{+7}$	7.35×10^{-8}	1.76×10^{-11}	0.84
LMP 15	$1.17\times10^{+6}$	3.59×10^{-7}	1.21×10^{-11}	0.85
LMP 20	$1.57\times10^{+7}$	5.18×10^{-8}	3.37×10^{-11}	0.77

Figure 5 shows the frequency-dependent plot for the permittivity of Li_3PO_4-MMT-PVDF composite samples. The parameters were calculated from the real and imaginary part of the impedance. The real part of complex permittivity is the dielectric constant (ε'), while the imaginary part is the dielectric loss (ε''). In a low-frequency range, a very strong dispersion is observed in both the real and imaginary parts of permittivity. Both of these parts increase with decreasing frequency, which is attributed to the high contribution of charge accumulation at the electrode–electrolytes interfaces (Baskaran et al., 2004). Permittivity is followed by nearly frequency-independent behavior, and it attains a constant limiting value at a higher-frequency range. At higher frequencies, rapid electric field reversal causes a decrease in polarization due to charge accumulation. Therefore, there is no excess ion diffusion in the direction of the field, which results in a decrease in both real and imaginary parts of permittivity.

With the addition of MMT up to 15 wt%, the magnitude of both permittivity aspects increased, and the curve shifted toward a higher frequency. Upon adding MMT there is an increase in the amount of free space that may increase bipolar orientation and diffusion of the charge carrier. The increase of mobility is reflected by the increase of permittivity strength as well as the shift of both permittivity curves toward a higher frequency. However, with the further addition of 20 wt% MMT, the decrease in the amount of conducting ions resulted in a decrease in both real

and imaginary permittivity. Table 2 lists some values of both the dielectric constant and dielectric loss at several frequencies.

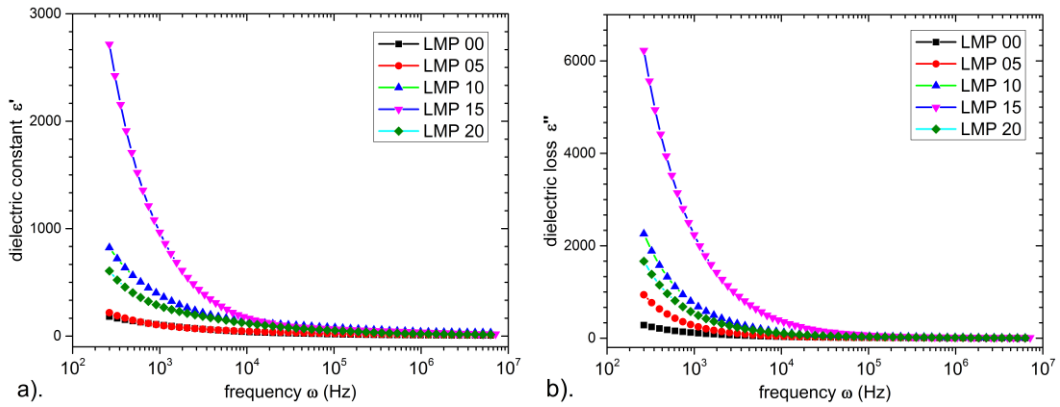

Figure 5 Frequency-dependent plots of permittivity for Li_3PO_4-MMT-PVDF composite samples with 0, 5, 10, 15, and 20 wt% of montmorillonite (MMT) additions

Table 2 List of the dielectric-constant and dielectric-loss values of Li_3PO_4-MMT-PVDF composite samples at several frequencies

Frequency	Dielectric constant			Dielectric loss		
	60 Hz	10 kHz	1 MHz	60 Hz	10 kHz	1 MHz
LMP 00	152.1	20.8	6.1	209.9	13.4	1.5
LMP 05	166.1	26.9	9.8	632.4	15.5	1.9
LMP 10	636.5	85.2	31.2	1580.1	48.1	6.2
LMP 15	2032.1	74.9	18.5	4676.9	92.1	9.6
LMP 20	455.8	59.3	13.6	1151.7	35.8	4.1

4. CONCLUSION

Li_3PO_4-MMT-PVDF composites were synthesized by mechanical blending with various MMT compositions. The XRD spectral data indicated that all the samples were composed mainly of γ-Li_3PO_4 crystal, with a small amount of $H_1Al_1Si_2O_6$ spectra in the samples with MMT additions. The SEM micrographs show that surface roughness decreased with MMT additions up to 15 wt%. Samples with a 15 wt% MMT addition issued a different response in impedance spectra, reflected by a spike in the lower-frequency region, and these samples attained the highest DC-conductivity value of 3.59×10^{-7} S/cm. This value is higher by two orders of magnitude than that of the sample with no MMT additions. The value of AC-conductivity parameters of higher-frequency slopes reveals that the long-range drift of ions may be one of the sources of ion conduction in the Li_3PO_4-MMT-PVDF system with MMT additions. An addition of MMT up to 15 wt% is believed to increase the mobile ions and free space in the sample, which is reflected by the increase of permittivity and the shift toward a higher frequency.

5. ACKNOWLEDGEMENT

We would like to thank to our colleagues at The Center for Science and Technology of Advanced Materials in BATAN as well as those from the Department of Metallurgy and Materials Engineering at Universitas Indonesia. This work was funded by the Indonesian Ministry of Research, Technology, and Higher Education of Republic of Indonesia.

6. REFERENCES

Baskaran, R., Selvasekarapandian, S., Hirankumar, G., 2004. Dielectric and Conductivity Relaxations in PVAc based Polymer Electrolytes. *Ionics*, Volume 10(1), pp. 129–134

Chilaka, N., Ghosh, S., 2014. Dielectric Studies of Poly (Ethylene glycol)-Polyurethane/Poly (Methylmethacrylate)/Montmorillonite Composite. *Electrochimica Acta*, Volume 134, pp. 232–241

Deka, M., Kumar, A., 2011. Electrical and Electrochemical Studies of Poly(Vinylidene Fluoride)–Clay Nanocomposite Gel Polymer Electrolytes for Li-ion Batteries. *Journal of Power Sources*, Volume 196(3), pp. 1358–1364

Fergus, J.W., 2010. Ceramic and Polymeric Solid Electrolytes for Lithium-ion Batteries. *Journal of Power Sources*, Volume 195(15), pp. 4554–4569

He, K., Zu, C., Wang, Y., Han, B., Yin, X., Zhao, H., Liu, Y., Chen, J., 2014. Stability of Lithium Ion Conductor NASICON Structure Glass Ceramic in Acid and Alkaline Aqueous Solution. *Solid State Ionics*, Volume 254, pp. 78–81

Jodi, H., Supardi, Kartini, E., Zulfia, A., 2016. Synthesis and Electrochemical Characterization of Li_3PO_4 for Solid State Electrolytes. *Indonesian Journal of Materials Science*, Volume 18(1), pp. 1–8

Jonscher, A.K., 1977. The Universal Dielectric Response. *Nature*, Volume 267(5613), pp. 673–679

Kartini, E., Honggowiranto, W., Supardi, Jodi, H., Jahya, A.K., Wahyudianingsih, 2014. Synthesis and Characterization of New Solid Electrolyte Layer $(Li_2O)_x$ $(P_2O_5)_y$. *In:* Adams, S., Kawamura, J. (Eds.), Proceedings of the 14th Asian Conference on Solid State Ionics, Singapore, Research Publishing, pp. 163–173

Kotobuki, M., 2012. The Current Situation and Problems of Rechargeable Lithium-ion Batteries. *The Open Electrochemistry Journal*, Volume 4, pp. 28–35

Lepley, N.D., Holzwarth, N.A.W., 2012. Computer Modeling of Crystalline Electrolytes: Lithium Thiophosphates and Phosphates. *Journal of the Electrochemical Society*, Volume 159 (5), pp. A538–A547

Nur I.P.A., Kartini, E., Prayogi, L.D., Faisal, M., Supardi, 2016. Crystal Structure Analysis of Li_3PO_4 Powder Prepared by Wet Chemical Reaction and Solid State Reaction by using X-Ray Diffraction (XRD). *Ionics*, Volume 22(7), pp. 1051–1057

Pradhan, D.K., Choudhary, R.N.P., Samantaray, B.K., 2008. Studies of Dielectric Relaxation and AC Conductivity Behavior of Plasticized Polymer Nanocomposite Electrolytes. *International Journal of Electrochemical Science*, Volume 3, pp. 597–608

Quartarone, E., Mustarelli, P., 2011. Electrolytes for Solid-state Lithium Rechargeable Batteries: Recent Advances and Perspectives. *Chemical Society Reviews*, Volume 40(5), pp. 2525–2540

Raguenet, B., Tricot, G., Silly, G., Ribes, M., Pradel, A., 2012. The Mixed Glass Former Effect in Twin-roller Quenched Lithium Borophosphate Glasses. *Solid State Ionics*, Volume 208, pp. 25–30

Ribeiro, J.F., Sousa, R., Carmo, J.P., Gonçalves, L.M., Silva, M.F., Silva, M.M., Correia, J.H., 2012. Enhanced Solid-state Electrolytes Made of Lithium Phosphorous Oxynitride Films. *Thin Solid Films*, Volume 522, pp. 85–89

Sahu, G., Lin, Z., Li, J., Liu, Z., Dudney, N., Liang, C., 2014. Air-Stable, High-Conduction Solid Electrolytes of Arsenic-Substituted Li_4SnS_4. *Energy & Environmental Science*, Volume 7(3), pp. 1053–1058

Sakurai, Y., Sakuda, A., Hayashi, A., Tatsumisago, M., 2011. Preparation of Amorphous Li_4SiO_4–Li_3PO_4 Thin Films by Pulsed Laser Deposition for All-solid-state Lithium Secondary Batteries. *Solid State Ionics*, Volume 182(1), pp. 59–63

Senevirathne, K., Day, C.S., Gross, M.D., Lachgar, A., Holzwarth, N.A.W., 2013. A New Crystalline LiPON Electrolyte: Synthesis, Properties, and Electronic Structure. *Solid State Ionics*, Volume 233, pp. 95–101

Takahashi, C., Shirai, T., Hayashi, Y., Fuji, M., 2013. Study of Intercalation Compounds using Ionic Liquids into Montmorillonite and their Thermal Stability. *Solid State Ionics*, Volume 241, pp. 53–61

Yi, E., Wang, W., Mohanty, S., Kieffer, J., Tamaki, R., Laine, R.M., 2014. Materials that can Replace Liquid Electrolytes in Li Batteries: Superionic Conductivities in $Li_{1.7}Al_{0.3}Ti_{1.7}Si_{0.4}P_{2.6}O_{12}$ Processing Combustion Synthesized Nanopowders to Free-Standing Thin Films. *Journal of Power Sources*, Volume 269, pp. 577–588